High Performance Direct Torque Control of Induction Motor Drives: Problems and Improvements

Nik Rumzi Nik Idris
UTM-PROTON Future Drive Laboratory,
Universiti Teknologi Malaysia
Johor, Malaysia.
nikrumzi@fke.utm.my

Tole Sutikno
Department of Electrical Engineering,
Univasitas Ahmad Dahlan,
Yogjakarta, Indonesia.
tole@ee.uad.ac.id

***Abstract*—This paper presents some of the main problems, as well as their root causes, of Direct Torque Control (DTC) 3-phase induction motor drive. The high torque ripple in DTC drive due to the hysteresis controller inevitably becomes worst with the discrete implementation of the drive system. The hysteresis controller also causes variable switching frequency that depends on operating conditions, especially the speed. The simplification used in stator flux expression for voltage vectors selection in flux control results in a poor flux regulation at low speed. To overcome these problems, techniques that have been implemented at UTM-PROTON Future Drive Laboratory (UPFDL) are presented and described. Some experimental results obtained from the previous works are also presented and discussed.**

Keywords—component; formatting; style; styling; insert (key words)

I. INTRODUCTION

Direct torque Control (DTC) and Field-oriented Control (FOC) are the two most widely used control techniques for induction motor drives for high performance applications. Each control technique has its own advantages and drawbacks. In general, the choice between the two depends on the requirements of the applications. In terms of torque dynamic responses, both techniques give excellent performance, which is comparable, if not better, than the DC motor drives counterpart. DTC for induction motor drive was introduced by Takahashi [1] and Depenbrock [2]. The latter, however, produces low harmonics stator current with low switching frequency and thus more suitable for high power applications; it is also widely known as Direct-self Control (DSC). DTC by Takahashi on the other hand, switches at relatively higher switching frequency and produces circular flux locus, thus results in an almost sinusoidal stator current waveforms.

Since the introduction of DTC, there have been several different proposals in its implementations, with the aim of removing the major problems associated with it, namely the high torque ripple and variable switching frequency. The root cause to these problems is mainly due to the use of hysteresis controllers for the torque and flux regulations. In DTC of induction motor, it is common practice to neglect the stator resistance drop in the stator flux equation in order to simplify the selection of voltage vectors for the stator flux control. By doing so, flux regulation at low speed becomes problematic. This paper will highlight these common problems and discuss their root causes. The paper will also present some of the methods to solve them, which have been published and implemented at UTM-PROTON Future Drive Laboratory (UPFDL), Universiti Teknologi Malaysia. Hence it should be noted that there are, of course, other methods and techniques that can be used to solve these problems which can be found in the literatures. And, it should also be noted that the problems associated with DTC are not only limited to the ones mentioned in this paper. A comprehensive review on DTC, for example, can be obtained from several review papers [4][9].

The organization of this paper is as follows. In Section II, the fundamental knowledge and principles of DTC are presented. The root causes to the 3 major problems, namely the high torque ripple, variable switching frequency and poor flux regulation at low speed are presented in Section III. Methods on how to solve these problems and some experimental results (implemented at UPFDL), are next presented in Section IV. Finally, a conclusion is presented in Section V.

II. DIRECT TORQUE CONTROL: PRINCPLES OF OPERATION

A. Induction motor model

The induction motor can be described in a compact form using space vector equations. The equations can be expressed in various reference frames, and if expressed in general reference frame rotating at a speed ω_g, the equations of a squirrel cage 3-phase induction motor can be written as,

$$\begin{aligned} \boldsymbol{v}_s^g &= R_s \boldsymbol{i}_s^g + \frac{d\boldsymbol{\psi}_s^g}{dt} + j\omega_g \boldsymbol{\psi}_s^g \\ 0 &= R_r \boldsymbol{i}_r^g + \frac{d\boldsymbol{\psi}_r^g}{dt} + j\left(\omega_g - \omega_r\right)\boldsymbol{\psi}_r^g \\ \boldsymbol{\psi}_s^g &= L_s \boldsymbol{i}_s^g + L_m \boldsymbol{i}_r^g \\ \boldsymbol{\psi}_r^g &= L_r \boldsymbol{i}_r^g + L_m \boldsymbol{i}_s^g \end{aligned} \quad (1)$$

978-1-5386-0549-3/17/$31.00 ©2017 IEEE

In these equations, $\boldsymbol{v}_s^g$ and $\boldsymbol{i}_s^g$ are the stator voltage and current space vectors, and $\boldsymbol{i}_r^g$ is the rotor current space vector. The stator flux and rotor flux space vectors are represented by $\boldsymbol{\psi}_s^g$ and $\boldsymbol{\psi}_r^g$ respectively. These space vectors are all expressed in general rotating frame indicated by the superscript 'g'. The parameters of the machine are given by L_s – stator self-inductance, L_r – rotor self-inductance, and R_s and R_r the stator and rotor resistances respectively. The algorithm for flux and torque control in DTC is mainly based on stationary reference frame whereby $\omega_g = 0$.

B. *Flux and Torque Control*

A decoupled control between the torque and flux in induction motor is not as simple as that of DC motor, because the rotor field is induced from the rotating field generated on the stator. Thus the displacement between the two components highly depends on the operating conditions, such as speed and load torque. In general, DTC and FOC techniques are introduced so that a decoupled control in torque and flux components can be established. In FOC drives, the stator currents are resolved into its flux and torque components in a rotating reference frame fixed to a field flux. The torque and flux are indirectly controlled via the stator currents, thus the implementation of FOC normally requires current controlled schemes and/or pulse width modulator. On the other hand, in DTC, the torque and flux components are controlled by appropriate selection of suitable switching patterns of the voltage source inverter (VSI) while keeping the torque and flux within their hysteresis bands. In contrast to FOC, no current controlled scheme and pulse width modulator are required. A schematic diagram of DTC induction motor drive is shown in Fig. 1. It consists of a pair of hysteresis controllers (for the flux and torque controls), a look-up table for voltage vectors selection, and torque and stator flux estimator.

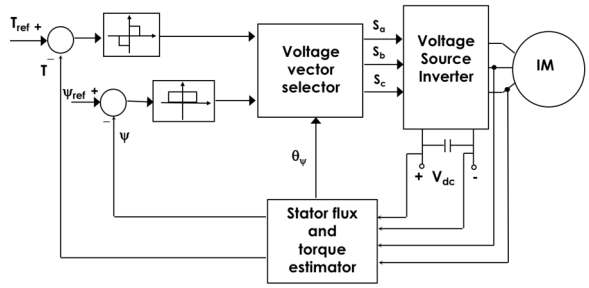

Fig. 1 Direct Torque Control of induction motor drive

The influence of the selected voltage vectors on the stator flux can be understood by considering the simplified stator voltage space vector equations of the induction motor in stationary reference frame ($\omega_g = 0$). If the stator resistance drop is neglected, and over a small period of time (such that $d\boldsymbol{\psi}_s \equiv \Delta\boldsymbol{\psi}_s$ and $dt \equiv \Delta t$), the change in stator flux can be written, based on the stator voltage equation in (1), as

$$\Delta\boldsymbol{\psi}_s = \boldsymbol{v}_s \Delta t. \tag{2}$$

As can be seen from (2) that the stator flux can be directed to follow a desired locus by carefully applying suitable voltage vectors over a small period of time Δt. For a two-level, 3-phase VSI, eight possible switching patterns, leading to eight possible voltage vectors, must be carefully selected to control the stator flux within its hysteresis band. It can be shown that a voltage vector of a 2-level 3-phase VSI can be written in terms of the switching status of each leg as follows:

$$\boldsymbol{v}_s = \frac{2}{3} V_{dc}\left(S_a + S_b e^{j2\pi/3} + S_c e^{j4\pi/3}\right) \tag{3}$$

In (3), S_a, S_b and S_c are the switching status for each leg of the 3-phase VSI; it is 1 when the upper switch of a leg is ON, and 0 when the lower switch is ON. Based on (3), 6 active voltage vectors are shown in Fig. 2. The other two voltage vectors, which are zero vectors, are when either all upper switches ON or all lower switches ON (i.e. [000] or [111]).

The selection rule of the voltage vector for stator flux control is simplified by dividing the stator flux plane into 6 sectors, as shown in Fig. 3. Whenever the stator flux enters a new sector, a new set of voltage vectors will be used to increase or reduce the flux, according to (2). For instance, when in sector 3, as shown in the figure, with counter clockwise rotation, v_4 and v_5 are used to increase and reduce the flux within its hysteresis band respectively. The decision to increase or reduce the flux comes from the flux hysteresis controller, which is then fed to the voltage vector selector (or look-up table).

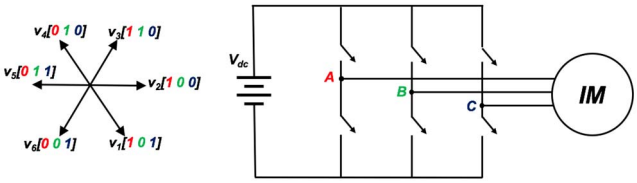

Fig. 2 3-phase VSI and possible voltage vectors.

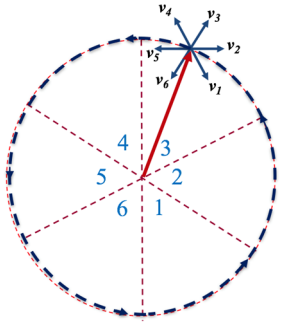

Fig. 3 Division of stator flux plane into 6 sectors

The selection of voltage vector to control the torque can be explained by considering the torque equation written in terms of stator and rotor flux magnitude, as given by (4).

$$T_e = \frac{3}{2}\frac{L_m}{\sigma L_s L_r}\psi_s \psi_r \sin\delta_{sr} \tag{4}$$

In this equation, δ_{sr} is the displacement angle between stator and rotor fluxes. Since the stator flux variation is within its hysteresis band, which is much smaller that its rated magnitude, it can be assumed that its magnitude, so too the rotor flux magnitude, are constant. Thus, torque can be conveniently controlled via δ_{sr} by selecting suitable voltage vectors. For instance, if the stator flux is located in sector 3, flux torque can be increased by selecting

v_4 or v_5. Selecting v_4 increases the flux, whereas selecting v_5 reduces the flux. On the other hand, if torque needs to be reduced, zero voltage vector is selected. By selecting zero voltage vector, stator flux will freeze (according to (2)) and rotor flux moves closer to the stator flux hence reducing δ_{sr}. Alternatively, reverse voltage vector can be used to rapidly reduce torque. Choosing reverse voltage vectors, however, causes a very high switching frequency and normally avoided in most cases.

Depending on the position of the flux, each voltage vector has different influence on the torque and flux components of the motor. With respect to the circular stator flux locus, these voltage vectors can be resolved into their tangential and radial components. The toque is influenced by the tangential components of the voltage vector, while the flux is influenced by radial components. As the flux rotates, the magnitudes of tangential and radial components of the voltage vector changes with stator flux position. Fig. 4 shows the tangential and radial components variation for voltage vector v_4 as the flux enters, reaches halfway, and leaves sector 3. When the flux in sector 3, voltage vectors v_4 and v_5 are used to increase and reduce the flux respectively. Both v_4 and v_5 will, at the same time, increase the torque. Upon entering sector 3, the radial component of v_4 (designated as $v_{4\beta}$) is very weak. On the other hand v_4 has a strong radial (torque) component (designated as $v_{4\alpha}$). The weakening followed by strengthening of radial component across a sector subsequently causes the stator flux droop starting at the beginning of a sector and ends somewhere in the middle of a sector; this is undesirable since it leads to deterioration in the stator currents and causes additional current harmonics [3]. The droop in flux is in fact due to the failure in stator flux regulation, as will be discussed in the next section.

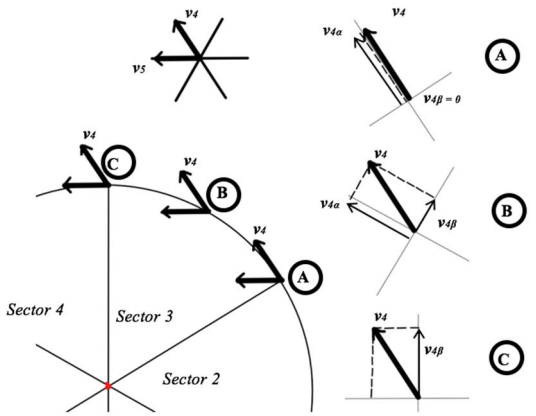

Fig. 4 Variation of torque and flux components of voltage vectors within sector 3.

III. Problems in Basic DTC

Even though DTC as proposed in [1] offers excellent torque dynamic, there are several problems normally associated with it. The root cause to these problems are mainly due to the use of hysteresis controllers for torque and flux regulations. The solutions to these problems, which normally leads to the removal of the hysteresis comparators, end up with improved versions of DTC but unfortunately, most of the time with increased complexity [4]. With the removal of hysteresis controllers, voltage vector look-up table is no longer required, instead reference stator voltage vector is generated and has to be synthesized; the most common solution is to use space vector modulator (SVM). However, this paper will only focus on the look-table based DTC. This section will give an overview to some of these problems and their root causes.

A. High torque ripple

Even though hysteresis controllers are known for their excellence dynamic performance, they, however, inevitably produces high ripple in the controlled variables. In ideal case with infinitesimal sampling time, the ripple of the torque is contained within the hysteresis band. In practice, with finite sampling time, the torque will exceed beyond the hysteresis band. Fig. 5(a) illustrate an ideal condition (zero sampling time) operation of a hysteresis comparator. In practical implementation, with sampling time t_{s1}, overshoot and undershoot situations are inevitable as illustrated by Fig.5(b). As the sampling becomes larger, so too are the overshoot and undershoot in torque, which is shown in Fig.5(c) whereby $t_{s2} > t_{s1}$. The worst case is when the undershoot in the torque error causes a faulty selection of reverse voltage vectors, that will further increase the torque ripple [5]. This happens when the hysteresis band is set too small relative to the sampling time, as shown in Fig. 6, which is obtained from experimental results of DTC drive on a ¼ hp induction motor. The red circles are instances of unintentional reverse voltage vectors selections.

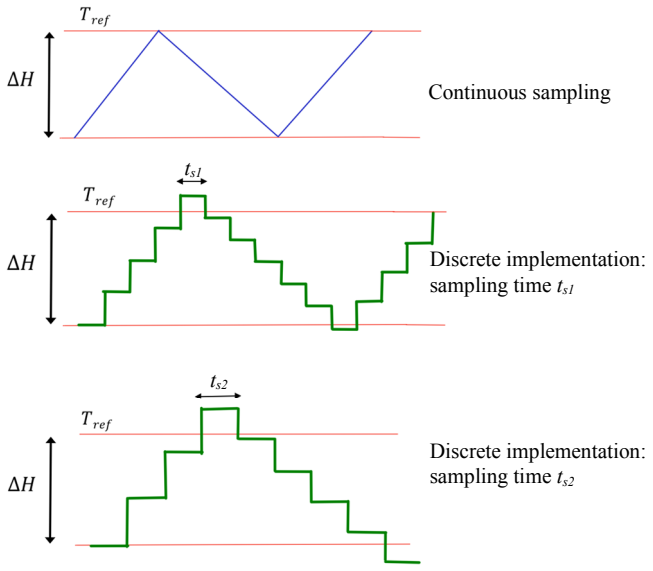

Fig. 5 Discrete implementation of hysteresis controller causes overshoot and undershoot in torque.

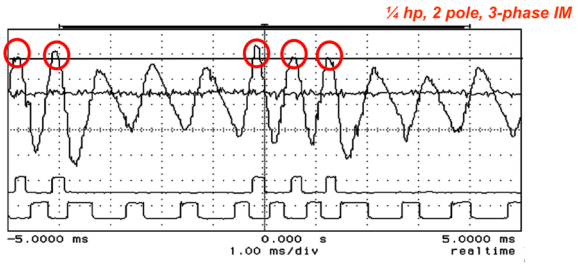

Fig. 6 Unintentional reverse voltage vector selections due to overshoot in torque. Top trace torque, bottom traces are the torque error status.

B. *Variable switching frequency*

The switching frequency of the inverter in mainly influenced by the switching of the torque hysteresis comparator [5]. Every time the torque error touches the upper and lower hysteresis bands, inverter switching pattern will change. The positive and negative torque slopes are given by [5]

$$\frac{dT_e^+}{dt} = -T_e\left(\frac{1}{\sigma\tau_s}+\frac{1}{\sigma\tau_r}\right)+\frac{3}{2}\frac{p}{2}\frac{L_m}{\sigma L_s L_r}(u_s - j\omega_r\psi_s)\cdot j\psi_r \quad (5a)$$

$$\frac{dT_e^-}{dt} = -T_e\left(\frac{1}{\sigma\tau_s}+\frac{1}{\sigma\tau_r}\right)-\frac{3}{2}\frac{p}{2}\frac{L_m}{\sigma L_s L_r}(j\omega_r\psi_s)\cdot j\psi_r \quad (5b)$$

Since the positive and negative slopes of the torque change with operating conditions, the speed (ω_r), so too is the switching frequency. The variable switching frequency condition is illustrated in Fig. 7, which shows a typical torque waveform at low and medium speed. The variable switching frequency is undesirable since it is unpredictable and thus making it difficult to select the frequency rating of the switching device. If the selection is made based on a worst-case condition, the devices might not be fully utilized since they will be operated below this value most of the time.

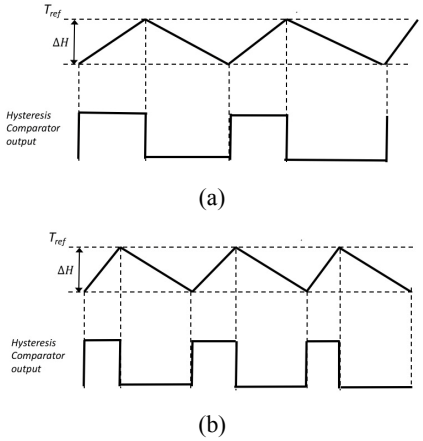

Fig. 7 Switching frequency at different speed (a) medium, (b) low

C. *Poor flux regulation at low and zero speed*

In controlling the flux, it is assumed that no net change in flux occur when zero voltage vectors are selected, this is in accordance with equation (2). In actual, without simplification to the stator voltage equation, the change in stator flux whenever active and zero voltage vectors are applied are given by (6) and (7), respectively.

$$\Delta\boldsymbol{\psi}_{s1} = (\boldsymbol{u}_s - \boldsymbol{i}_s R_s)\Delta t_1 \quad (6)$$

$$\Delta\boldsymbol{\psi}_{s2} = -\boldsymbol{i}_s R_s \Delta t_2 \quad (7)$$

In (6), Δt_1 is the duration in which active voltage vector is applied to increase the torque and Δt_2 is the duration of zero voltage vector to reduce the torque. Note that zero voltage vector causes a decrement in flux. Flux cannot be properly regulated within its hysteresis band if the flux decrement is larger than its increment, i.e. $\Delta\psi_{s1} < \Delta\psi_{s2}$, as shown in Fig. 8.

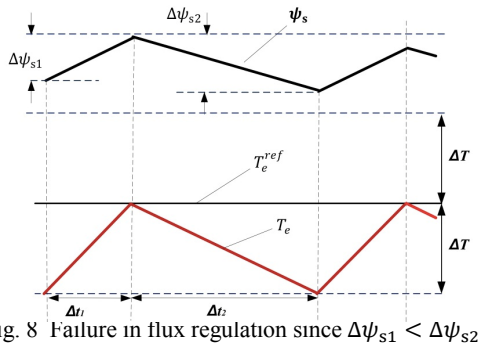

Fig. 8 Failure in flux regulation since $\Delta\psi_{s1} < \Delta\psi_{s2}$

If the drive is speed sensorless, the poor flux regulation has a detrimental effect to the speed estimation [6]. This happens when the speed estimator is tuned with the assumption that the flux is maintained at its rated value.

IV. Improvements in DTC

The improvements in DTC presented in this section is part of the methods which has been implemented at UPFDL. The objectives of the improvements are (1) to maintain a constant switching frequency, (2) to reduce the torque ripple, and (3) to improve flux regulation at low speed. It should be noted that the techniques which are used to overcome these problems are not limited to the ones presented in this paper. There are various other methods and techniques which can be adopted, but it is not the scope of this paper to discuss them here.

A. *Constant Switching Frequency Controller (CSFC)*

It has been discussed in the previous section that the high torque ripple and variable switching frequency problems are due to the employment of the torque hysteresis controller. It was proposed in [5] that the hysteresis controller is replaced by the so called constant switching frequency controller (CSFC), which is depicted in Fig. 9.

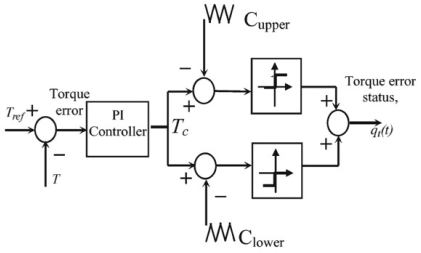

Fig. 9 Constant switching frequency controller (CSFC)

The controller has the same output pattern as the 3-level hysteresis controller (as given by (8)) and the switching

frequency of the 3-phase VSI is mainly determined by the frequency of the triangular wave.

$$T_{stat} = \begin{cases} 1, & T_c \geq C_{upper} \\ 0, & C_{lower} < T_c < C_{upper} \\ -1, & T_c \leq C_{lower} \end{cases} \quad (8)$$

To systematically design the PI controller, the torque loop has to be averaged and linearized, which is discussed in detailed in [5] and shown in Fig. 10. $C_{p\text{-}p}$ in the figure is the peak-peak of the triangular waves (upper and lower).

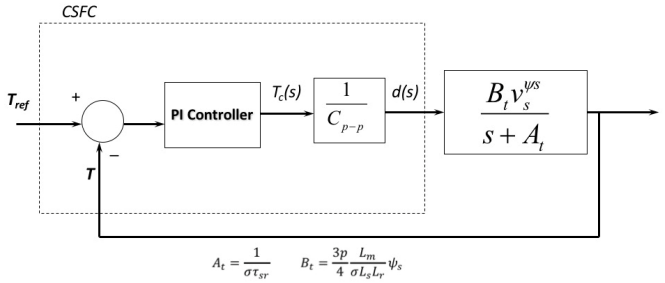

Fig. 10 Averaged and linearized torque loop [5]

Some of the experimental results performed on a ¼ hp 3-phase induction motor, showing the torque and frequency spectrum of the phase current in comparison with the hysteresis controller, are depicted in Fig. 11. Since the controller was implemented by a digital signal processor (dSPACE DS1102), its triangular frequency is limited by the sampling frequency, which is at 2.2 kHz (sampling frequency is 18 kHz); the switching frequency at 2.2 kHz can be observed from the frequency spectrum.

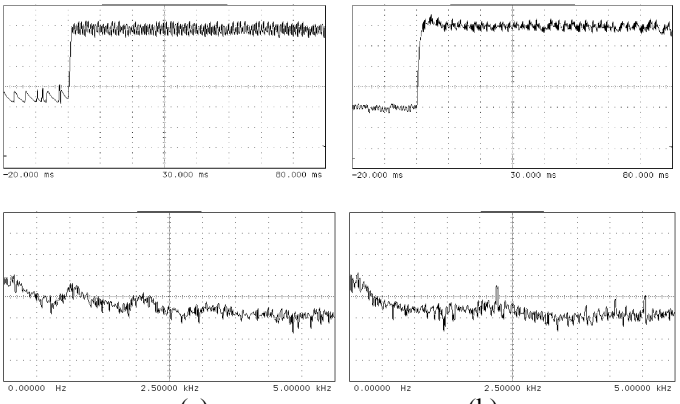

(a) (b)

Fig. 11 Step torque response and phase current frequency spectrum for (a) torque hysteresis controller, (b) torque CSFC with triangular frequency of 2.2 kHz [5]

In [7], the constraint on the switching frequency was removed by implementing the controllers using an FPGA device. In the implementation, not only the torque hysteresis controller, but the flux hysteresis controller is also being replaced with CSFC. Since there is no more constraint on the triangular frequency due to the DSP sampling, the switching frequency was increased to 10 kHz. Due to the higher switching frequency, torque ripple is further reduced, as shown in Fig. 12.

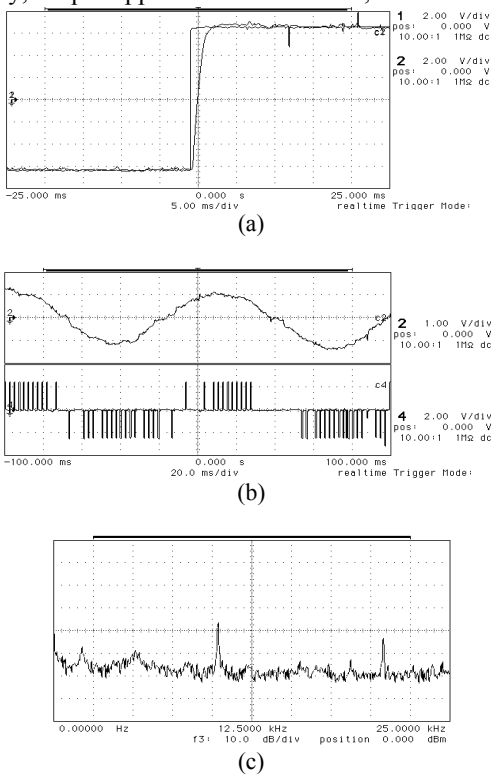

(a)

(b)

(c)

Fig. 12 Flux and torque CSFC implemented on a ¼ hp 3-phase induction motor (a) step torque response, (b) stator phase current and line voltage, (c) Frequency spectrum of stator current

B. Improved stator flux regulation at low speed

The improvement in flux regulation at low speed, can be accomplished by replacing the torque hysteresis controller with CSFC, as shown [6] and [8]. This is because with CSFC, higher and constant switching frequency at low speed is possible and thus the duration for zero vectors application is shortened, hence resulted in a smaller $\Delta\psi_{s2}$. Furthermore, with CSFC, the selection of reverse voltage vectors to reduce the torque (instead of zero voltage vectors) occurs naturally. With active voltage vectors, flux can be either increased or decreased. It is shown in [6][8] that with the improvement in stator flux regulation, the speed estimation based on Extended Kalman Filter (EKF) at low speed and start-up is significantly improved. The accuracy of the EKF based speed estimation depends on the tuning of the covariance matrices, which are optimized at rated flux. Fig. 13 and 14 show some of the experimental results obtained with the speed estimation performed by EKF technique, in comparison with the conventional method based on hysteresis controller. The drive system was implemented to a 1.5 kW 3-phase induction motor using dSPACE DS1104 as the main controller. Details on the implementation is given in [6] and [8]. In Fig. 13, a step speed from 10 rad/s to zero performed. With the torque hysteresis controller, the flux regulation fails and collapse and thus causes error in the estimated speed. However with CSFC, the flux is maintained at its rated value, which improves speed estimation. Fig. 14 shows a comparison between torque

hysteresis controller and CSFC during start-up. Due to the incorrect speed estimation caused by poor flux regulation, DTC with torque hysteresis controller exhibits an initial current surge. Flux regulation completely fails at zero speed. DTC with CSFC, on the other hand, shows good start-up with rated flux maintained even at zero speed.

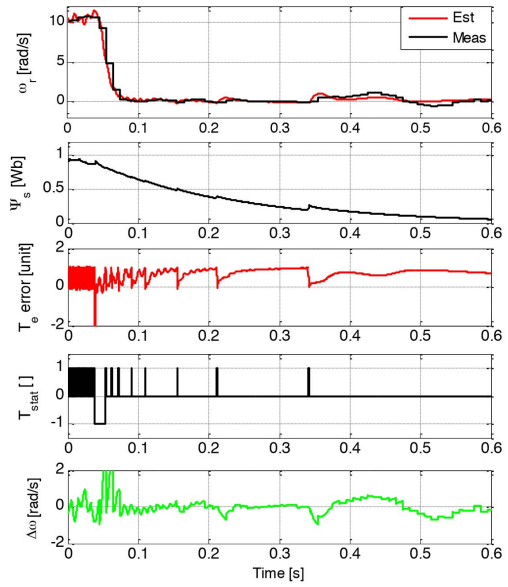

(a)

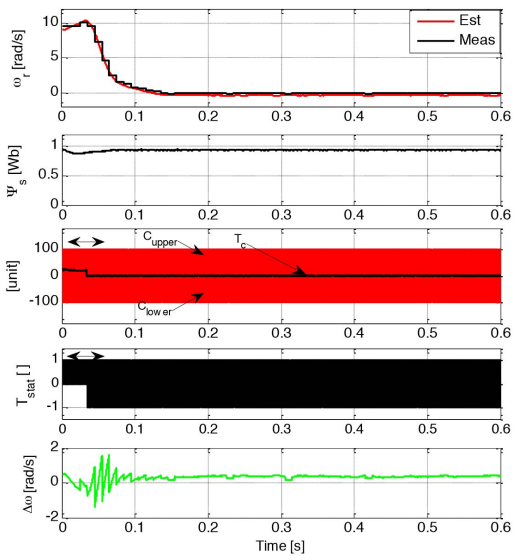

(b)

Fig 13. Speed, stator flux, torque, torque demand and stator phase current of the sensorless DTC drive utilizing (a) torque hysteresis controller, (b) Torque CSFC [6]

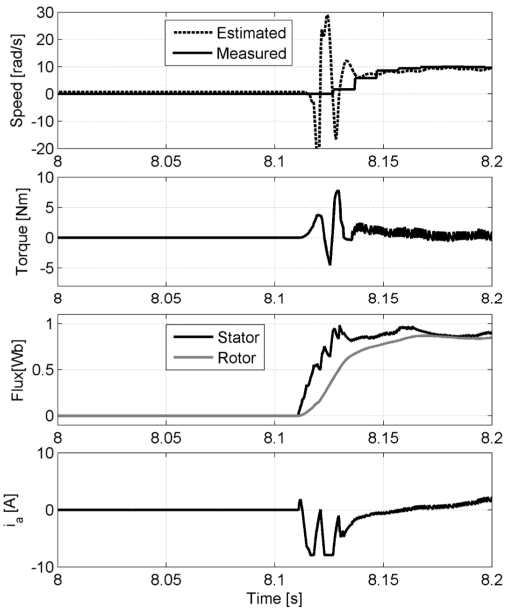

(a)

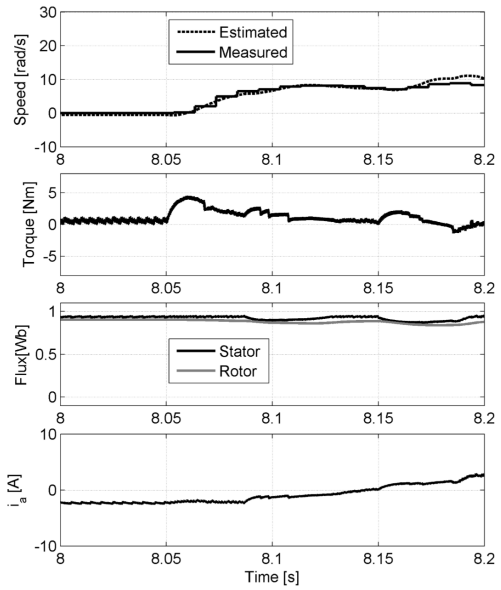

(b)

Fig. 14 Speed, torque flux and phase current during start-up (a) torque hysteresis controller, (b) CSFC [8]

V. CONCLUSIONS

In this paper, 3 major problems associated with DTC induction motor drives are presented and described; they are high torque ripple, variable switching frequency and poor flux regulation at low speed. Techniques that can be used to improve the performance of the DTC drive are also presented. It is shown that these problems are rooted from the torque hysteresis controller, and thus the performance of the DTC drive can be improved by replacing it with the CSFC. Finally, experimental results obtained from the previous work conducted at UPFDL

to overcome these problems showed that significant improvements in the drive performance were achieved.

VI. Acknowledgement

The authors would like to express gratitude to Ministry of Education (MOE) and Universiti Teknologi Malaysia (UTM) for the financial support provided under Research University Grant (RUG) Q.J130000.2523.18H07.

VII. References

[1] I. Takahashi, T. Noguchi, "A new quick-response and high-efficiency control strategy of an induction motor", *IEEE Trans. Ind. Appl.*, vol. IA-22, no. 5, pp. 820-827, Sep. 1986.

[2] M. Depenbrock, "Direct self-control (DSC) of inverter-fed induction machine", *IEEE Trans. Power Electron.*, vol. 3, no. 4, pp. 420-429, Oct. 1988.

[3] W.S.H. Wong and D. Holliday, "Minimisation of flux droop in direct torquecontrolled induction motor drives," IET Proceedings – Electric Power Applications, vol 151, no. 6, pp. 694-703, Dec. 2004.

[4] G. S. Buja and M. P. Kazmierkowski, "Direct torque control of PWM inverter-fed AC motors - a survey," *IEEE Trans. Ind. Electronics,* vol. 51, pp. 744-757, 2004.

[5] N. R. N. Idris and A. H. M. Yatim, "Direct torque control of induction machines with constant switching frequency and reduced torque ripple," *IEEE Trans. Ind. Electronics,* vol. 51, pp. 758-767, 2004

[6] I. Alsofyani and NRN Idris, "Lookup-Table-Based DTC of Induction Machines With Improved Flux Regulation and Extended Kalman Filter State Estimator at Low-Speed Operation", IEEE Transactions on Industrial Informatics, vol. 12, no. 4, pp. 1412-1425, May 2016

[7] NRN Idris, CL Toh and M Elbuluk, "A New Torque and Flux Controller for Direct Torque Control of Induction Machines", IEEE Transactions on Industry Applications, vol. 42, no. 6, pp: 1358 - 1366, 2006

[8] I. Alsofyani and NRN Idris, "Simple Flux Regulation for Improving State Estimation at Very Low and Zero Speed of a Speed Sensorless Direct Torque Control of an Induction Motor", IEEE Transactions on Power Electronics, vol. 31, no. 4, pp. 3027-3035, 2016

[9] D. Casadei, G. Serra, A. Tani and L. Zarri, "Direct Torque Control for induction machines: A technology status review", 2013 IEEE Workshop on Electrical Machines Design, Control and Diagnosis (WEMDCD), pp. 117-129, 2013